

**Contract No.:**

This manuscript has been authored by Savannah River Nuclear Solutions (SRNS), LLC under Contract No. DE-AC09-08SR22470 with the U.S. Department of Energy (DOE) Office of Environmental Management (EM).

**Disclaimer:**

The United States Government retains and the publisher, by accepting this article for publication, acknowledges that the United States Government retains a non-exclusive, paid-up, irrevocable, worldwide license to publish or reproduce the published form of this work, or allow others to do so, for United States Government purposes.

# High Temperature Hall-effect Investigations of Cd<sub>0.85</sub>Mn<sub>0.10</sub>Zn<sub>0.05</sub>Te Crystals

V. Kopach<sup>1</sup>, O. Kopach<sup>1</sup>, A. Kanak<sup>1</sup>, L. Shcherbak<sup>1</sup>, P. Fochuk<sup>1</sup>, A. E. Bolotnikov<sup>2</sup>, R. B. James<sup>3</sup>

<sup>1</sup> – Chernivtsi National University, Ukraine

<sup>2</sup> – Brookhaven National Laboratory, USA

<sup>3</sup> – Savannah River National Laboratory, USA

## ABSTRACT

High temperature Hall-effect investigations were used to study the change of the concentration and mobility of charge-carriers in Cd<sub>0.85</sub>Mn<sub>0.10</sub>Zn<sub>0.05</sub>Te and Cd<sub>0.85</sub>Mn<sub>0.10</sub>Zn<sub>0.05</sub>Te:In crystals grown by the vertical Bridgman technique. The Cd<sub>0.85</sub>Mn<sub>0.10</sub>Zn<sub>0.05</sub>Te and Cd<sub>0.85</sub>Mn<sub>0.10</sub>Zn<sub>0.05</sub>Te:In samples are characterized by optical and electrical measurements, and by IR microscopy. We determined that the value of the band gap increases with the Mn and Zn amount increasing in the Cd<sub>1-x-y</sub>Mn<sub>x</sub>Zn<sub>y</sub>Te crystals. We also show that after the high-temperature Hall-effect measurements performed under Cd overpressure, the resistivity of both crystals increases from 10<sup>4</sup> Ohm×cm to 10<sup>6</sup> Ohm×cm, and the amount and size of the Te inclusions decrease. According to the results of the high temperature Hall-effect investigations, the range of temperatures and Cd vapor pressures were established in which indium plays a major role and controls the concentration of charge carriers.

**Keywords:** CMZT, Bridgman technique, Hall measurements, inclusions, electrical properties.

## 1. INTRODUCTION

Investigations of Diluted Magnetic Semiconductors (DMSs) are proving to be a grand challenge in solid-state science. As non-magnetic semiconductors, which are doped with a few percent of magnetic elements (usually transition-metals), they are easily integrated with existing semiconductors. In addition, they have high spin-polarization. Anomalous Hall-effect is also another important property of DMSs, which has been studied to understand the differences from normal Hall-effect and its cause [1]. The first DMSs to be identified were II-VI semiconductor alloys like Zn<sub>1-x</sub>Mn<sub>x</sub>Te (ZMT) and Cd<sub>1-x</sub>Mn<sub>x</sub>Te (CMT) [2].

Our colleagues conducted Hall-effect measurements at 300-420 K on Cd<sub>0.9</sub>Mn<sub>0.1</sub>Te:In crystals [3]. All investigated samples possessed n-type conductivity. Their results showed that the electron mobility increased after the thermal treatment, whereas its concentration  $n$ , which is defined as  $n=1/eR_H$  (where  $e$  is an electron charge), decreased drastically. The high-temperature Hall-effect measurements of the HPBM-grown Cd<sub>0.95</sub>Zn<sub>0.10</sub>Te:In (CZT:In) samples in the Cd vapor displayed some differences in comparison with CdTe. The main difference is a lowered free-carriers concentration, plausibly caused by Zn atoms in the lattice [4]. The authors of [5] determined that substituting 5 mol% CdTe by ZnTe enables mass transport from Cd-rich charges and significantly modified the electrical properties of the Cd<sub>0.95</sub>Zn<sub>0.05</sub>Te crystals.

The authors [6] indicate that CMT crystals exhibit better in-depth and lateral uniformity than CZT crystals. These results confirm the theoretical expectations regarding the near-unity Mn segregation coefficient in CdTe (compared to that of Zn), giving CMT an advantage over CZT in terms of improved uniformity. Investigations of the temperature behavior of the devices also reveals the difference in the activation energy of the dark current mechanisms for CZT and CMT.

The authors [7] concluded that CdTe can be strengthened by alloying with Zn and weakened by alloying with Mn. The replacement of 5% of the Cd by Zn caused  $P_t$  (transition pressure) to increase by about 12.5%. On the other hand, replacement of 10% of Cd by Mn caused a similar decrease in  $P_t$ . In the former case the compressibility of pure ZnTe is 20% lower than that of CdTe, so that their results indicate a significant bowing of the compressibility from a straight-line projection between the end members, indicating that the effect occurs with small additions of Zn, and not just due to the nature of the Zn-Te bond. In both cases, the implication is that the CdTe bond can be stabilized by substitution of Zn and destabilized by substitution of Mn.

During this research we investigated the electrical properties of  $\text{Cd}_{0.85}\text{Mn}_{0.10}\text{Zn}_{0.05}\text{Te}$  crystals and compared the influence of the replacement of both Zn and Mn in the CdTe lattice. The influence of the indium donor on the CMZT crystals properties was also established.

## 2. EXPERIMENTS

The  $\text{Cd}_{0.85}\text{Mn}_{0.10}\text{Zn}_{0.05}\text{Te}$  and  $\text{Cd}_{0.85}\text{Mn}_{0.10}\text{Zn}_{0.05}\text{Te}:\text{In}$  ( $C_0(\text{In}) \sim 2 \times 10^{17} \text{ at/cm}^3$ ) single crystals were grown by the Vertical Bridgman method. High purity elements of Cd, Mn, Zn and Te are thoroughly mixed, melted, and heated above  $1130^\circ\text{C}$  for few hours. The crystal growth is done by slowly moving the melt through a controlled temperature gradient.

As-grown crystals had good crystalline quality, and the samples selected for measurements of the electrical properties were cut from different parts of the ingots. Cleaved samples were characterized by optical transmission spectroscopy, IR microscopy, high-temperature Hall-effect and current–voltage measurements. To perform the I–V characteristics measurements, two ohmic contacts were deposited onto the samples.

High-temperature Hall-effect measurements were carried on a custom-made system. A schematic of this equipment and part of the ampoule used for these measurements were presented earlier [8]. The furnace temperature was controlled by precision thermostats Maxthermo MX 5438, which was programmed by a computer. The sample temperature was determined by the upper zone of the furnace, and the temperature of the Cd component (e.g. its vapor pressure) was set by the lower zone. Hall-effect and electrical conductivity measurements were performed using six welded (tungsten wire) contacts. The samples with contacts were put into the ampoule.

## 3. RESULTS AND DISCUSSIONS

Figs. 1a and b display the as-grown  $\text{Cd}_{0.85}\text{Mn}_{0.10}\text{Zn}_{0.05}\text{Te}$  and  $\text{Cd}_{0.85}\text{Mn}_{0.10}\text{Zn}_{0.05}\text{Te}:\text{In}$  crystals, respectively. The obtained ingots had dimensions of 39 and 43 mm in length and 18 mm in diameter. The crystalline structure of the In-doped crystal was more homogeneous than that of  $\text{Cd}_{0.85}\text{Mn}_{0.10}\text{Zn}_{0.05}\text{Te}$ . According to [9]  $\text{Cd}_{0.9}\text{Mn}_{0.1}\text{Te}:\text{In}$  wafers from the ingot grown by vertical Bridgman technique have multiple twins paralleled to each other, while only one twin is observed in the wafer by Te solution technique. In our case no one samples had the twins, although we used vertical Bridgman method as basic. It may be explained by the influence of 5 mol% of Zn presence. However, it was shown in earlier research [10] that replacing 5 mol% Cd by Zn in CdTe enhances the twinning phenomenon, which is expected as due to the ionicity of the crystal increase. In our case neither addition of Mn (10 mol. %) nor addition of Zn (5 mol. %) led to the twinning in the obtained crystals.

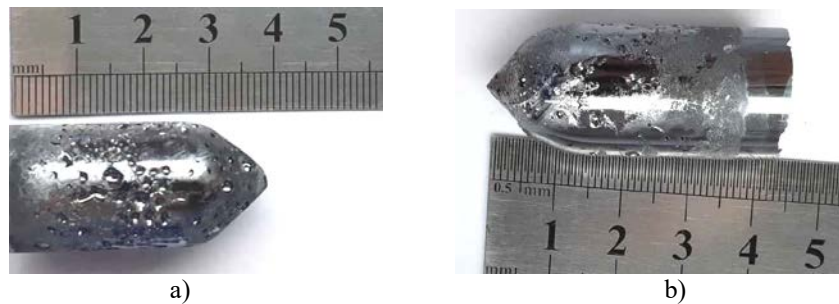


Figure 1. Photographs of as-grown  $\text{Cd}_{0.85}\text{Mn}_{0.10}\text{Zn}_{0.05}\text{Te}$  (a) and  $\text{Cd}_{0.85}\text{Mn}_{0.10}\text{Zn}_{0.05}\text{Te}:\text{In}$  (b) ingots.

Both types of crystals were investigated by optical (IR observation and transmission spectra) and electrical (current–voltage) measurements at room temperature and Hall-effect measurements at high-temperature. Corresponding IR micrographs of the as-grown  $\text{Cd}_{0.85}\text{Mn}_{0.10}\text{Zn}_{0.05}\text{Te}$  and  $\text{Cd}_{0.85}\text{Mn}_{0.10}\text{Zn}_{0.05}\text{Te}:\text{In}$  samples are shown in Figs. 2a and c. Using a layer-by-layer IR scanning technique and 3D modeling, a uniform distribution of the Te inclusions was observed for all samples along the entire length (Figs. 3a and 3b). Spherical inclusions with a diameter of 8 to 16  $\mu\text{m}$  were rarely observed in the as-grown  $\text{Cd}_{0.85}\text{Mn}_{0.10}\text{Zn}_{0.05}\text{Te}$  samples (the insert in Fig. 3c), and small inclusions with a diameter of 1  $\mu\text{m}$  to 5  $\mu\text{m}$  were found in the as-grown  $\text{Cd}_{0.85}\text{Mn}_{0.10}\text{Zn}_{0.05}\text{Te}:\text{In}$  samples (the insert in Fig. 3d).

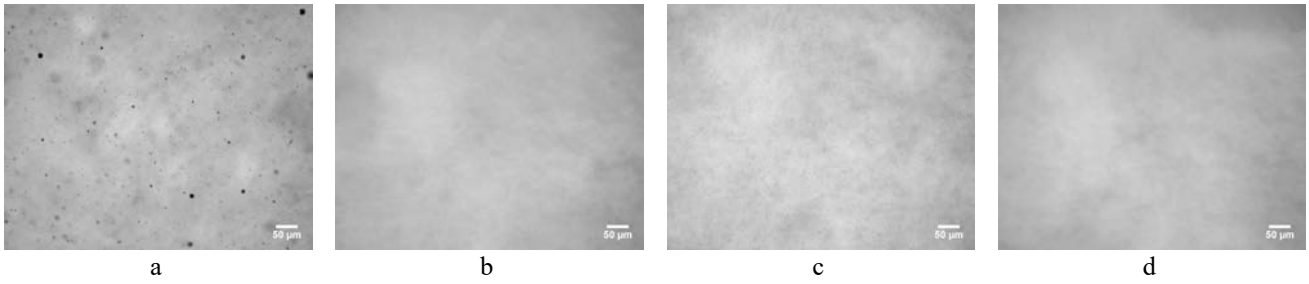


Figure 2. IR-transmission images of the  $\text{Cd}_{0.85}\text{Mn}_{0.10}\text{Zn}_{0.05}\text{Te}$  (a, b) and  $\text{Cd}_{0.85}\text{Mn}_{0.10}\text{Zn}_{0.05}\text{Te}:\text{In}$  (c, d) samples; a) and c) images of the as grown samples; b) and d) images of the same samples after the high-temperature Hall-effect measurements.

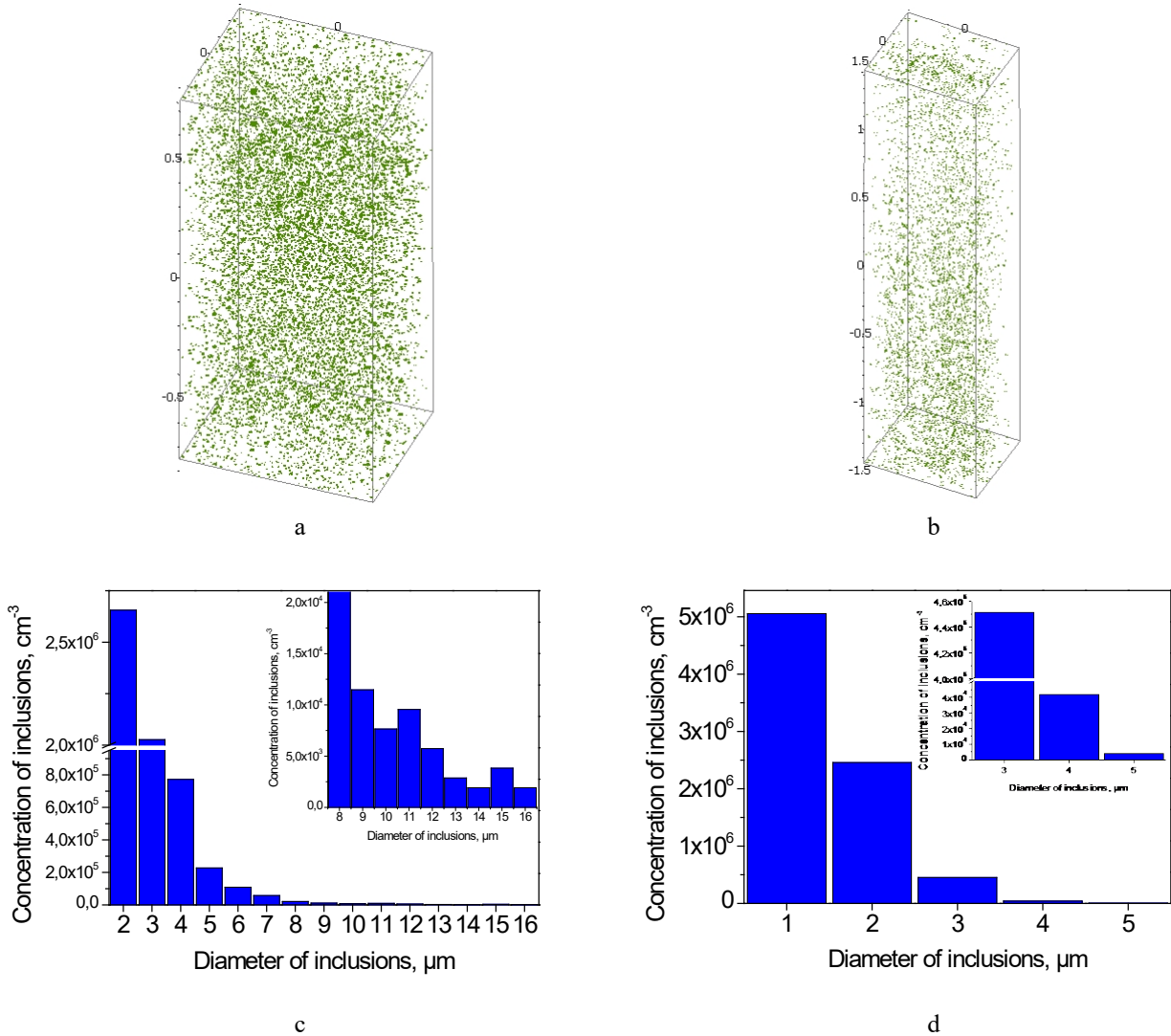


Figure 3. 3D model of the inclusions in as-grown  $\text{Cd}_{0.85}\text{Mn}_{0.10}\text{Zn}_{0.05}\text{Te}$  (a) and  $\text{Cd}_{0.85}\text{Mn}_{0.10}\text{Zn}_{0.05}\text{Te}:\text{In}$  (b) crystals; histograms of the sizes and concentrations of inclusions for  $\text{Cd}_{0.85}\text{Mn}_{0.10}\text{Zn}_{0.05}\text{Te}$  (c) and  $\text{Cd}_{0.85}\text{Mn}_{0.10}\text{Zn}_{0.05}\text{Te}:\text{In}$  (d). Here, the distributions were measured after the high-temperature Hall-effect measurements; the inserts in the plots show the results for as-grown crystals.

Changes in the defects were observed after the high temperature Hall-effect investigations, namely, the sizes of the Te inclusions in both crystals had decreased. Figs. 2b and d show IR transmission images of the  $\text{Cd}_{0.85}\text{Mn}_{0.10}\text{Zn}_{0.05}\text{Te}$  and  $\text{Cd}_{0.85}\text{Mn}_{0.10}\text{Zn}_{0.05}\text{Te}:\text{In}$  samples, correspondingly, after the annealing at  $P_{\text{Cd}}$  during the Hall-effect measurements. In this case no Te inclusions are seen on this spatial scale. Figs. 3c and d illustrate more clearly the decrease of the size and

the concentration of Te inclusions in samples after the high-temperature annealing. According to [11] the size of Te inclusions in  $\text{Cd}_{0.97}\text{Zn}_{0.03}\text{Te}$  can be successfully reduced by Cd-rich annealing at temperatures higher than  $660^\circ\text{C}$ ; and it was found that the Te inclusions contained practically pure Te. It was noted [11] that complete elimination of the remaining spots did not occur even after 24 h of Cd-rich annealing at  $1000^\circ\text{C}/870^\circ\text{C}$ .

Fig. 4 shows typical transmission spectra of an as-grown  $\text{Cd}_{0.85}\text{Mn}_{0.10}\text{Zn}_{0.05}\text{Te}$  sample compared with the data of our previous work [12, 13]. The band gap of the  $\text{Cd}_{0.85}\text{Mn}_{0.10}\text{Zn}_{0.05}\text{Te}$  sample was estimated to be about 1.63 eV, while we found in [12] the values of 1.74 eV and 1.89 eV for  $\text{Cd}_{0.75}\text{Mn}_{0.20}\text{Zn}_{0.05}\text{Te}$  and  $\text{Cd}_{0.65}\text{Mn}_{0.30}\text{Zn}_{0.05}\text{Te}$  crystals, respectively (Fig. 4a). The obtained values of the band gap show a reasonable linear behavior as a function of the atomic fraction of Mn, which is shown in the insert of Fig. 4a. The data follow the relation:

$$E_g = 1.49 + 1.30x \quad (R^2 = 0.98) \quad (1)$$

The authors in [14] also proposed the linear dependence of  $E_g$  vs. Mn content in  $\text{Cd}_{1-x}\text{Mn}_x\text{Te}$  crystals, and they estimated  $E_g$  for  $\text{Cd}_{0.90}\text{Mn}_{0.10}\text{Te}$  crystal as 1.6 eV. The band gap of the  $\text{Cd}_{0.85}\text{Mn}_{0.10}\text{Zn}_{0.05}\text{Te}$  sample is 0.03 eV higher, which is due to the Zn addition in our crystals.

As seen in Fig. 4b, the value of band gap increases from 1.63 eV to 1.67 eV [13] as the amount of Zn increases from 0.05 to 0.10. These results show an  $E_g$  dependence on the Mn and Zn concentrations.

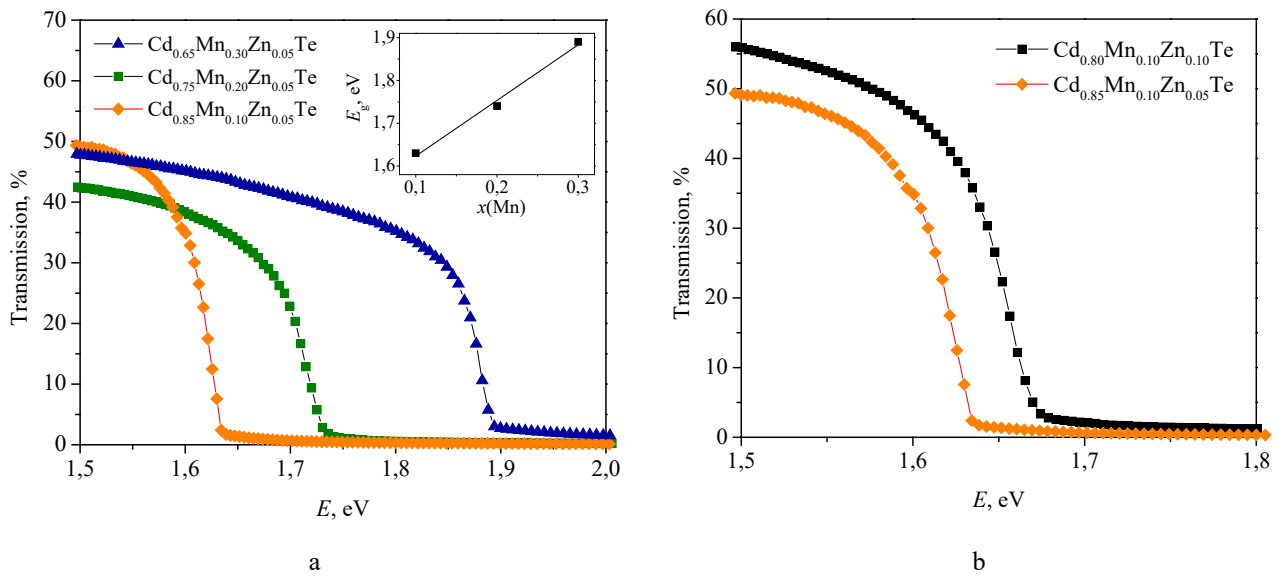


Figure 4. Typical transmission spectra of as-grown  $\text{Cd}_{0.85}\text{Mn}_{0.10}\text{Zn}_{0.05}\text{Te}$ ,  $\text{Cd}_{0.75}\text{Mn}_{0.20}\text{Zn}_{0.05}\text{Te}$  [12] and  $\text{Cd}_{0.65}\text{Mn}_{0.30}\text{Zn}_{0.05}\text{Te}$  [12] samples (a), and of as-grown  $\text{Cd}_{0.85}\text{Mn}_{0.10}\text{Zn}_{0.05}\text{Te}$  and  $\text{Cd}_{0.80}\text{Mn}_{0.10}\text{Zn}_{0.10}\text{Te}$  [13] samples (b). Insert in (a) represents the band gap of  $\text{Cd}_{0.95-x}\text{Mn}_x\text{Zn}_{0.05}\text{Te}$  crystals as a function of Mn content.

The electrical measurements gave the value of the initial resistivity of the investigated as-grown samples to be above  $10^4 \text{ Ohm}\times\text{cm}$  (the same order for other  $\text{Cd}_{1-x-y}\text{Mn}_x\text{Zn}_y\text{Te}$  crystals in [12, 13]). However, the resistivity of both crystals increased to  $6.8\times 10^6 \text{ Ohm}\times\text{cm}$  for  $\text{Cd}_{0.85}\text{Mn}_{0.10}\text{Zn}_{0.05}\text{Te}$  and to  $2.5\times 10^6 \text{ Ohm}\times\text{cm}$  for  $\text{Cd}_{0.85}\text{Mn}_{0.10}\text{Zn}_{0.05}\text{Te}:\text{In}$  samples after performing the high-temperature Hall-effect measurements under Cd overpressure. Fig. 5 shows a linear behavior of both I-V dependencies over a wide range of applied voltage.

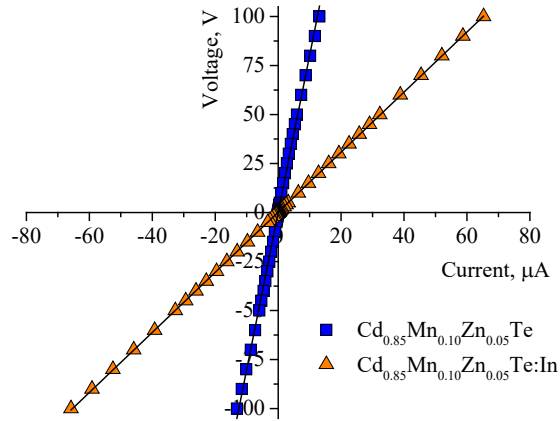


Figure 5. Current–voltage characteristics of  $\text{Cd}_{0.85}\text{Mn}_{0.10}\text{Zn}_{0.05}\text{Te}$  and  $\text{Cd}_{0.85}\text{Mn}_{0.10}\text{Zn}_{0.05}\text{Te:In}$  samples at room temperature after the high-temperature Hall-effect measurements.

A change of charge-carrier concentration during a series of heating-cooling cycles (thermocycling) was observed in  $\text{Cd}_{0.85}\text{Mn}_{0.10}\text{Zn}_{0.05}\text{Te}$  and  $\text{Cd}_{0.85}\text{Mn}_{0.10}\text{Zn}_{0.05}\text{Te:In}$  during the process of the high-temperature Hall-effect measurements. As we can see from Figs. 6 (a-b), the charge-carrier concentration was highest for both samples at the start of the measurements (Region I, blue points). For the undoped crystal  $\lg [e^-]$  gradually increases from 15 to 17, while the electron concentration in the  $\text{Cd}_{0.85}\text{Mn}_{0.10}\text{Zn}_{0.05}\text{Te:In}$  (black points) increases from 16 and adopts a stable value at level  $\sim 17$  during the heating at  $P_{\text{Cd}}$ , max up to  $600^\circ\text{C}$ . Such a difference between the samples is probably due to the dopant of indium whose concentration was  $2 \times 10^{17}$  at/cm<sup>3</sup> in the  $\text{Cd}_{0.85}\text{Mn}_{0.10}\text{Zn}_{0.05}\text{Te:In}$ .

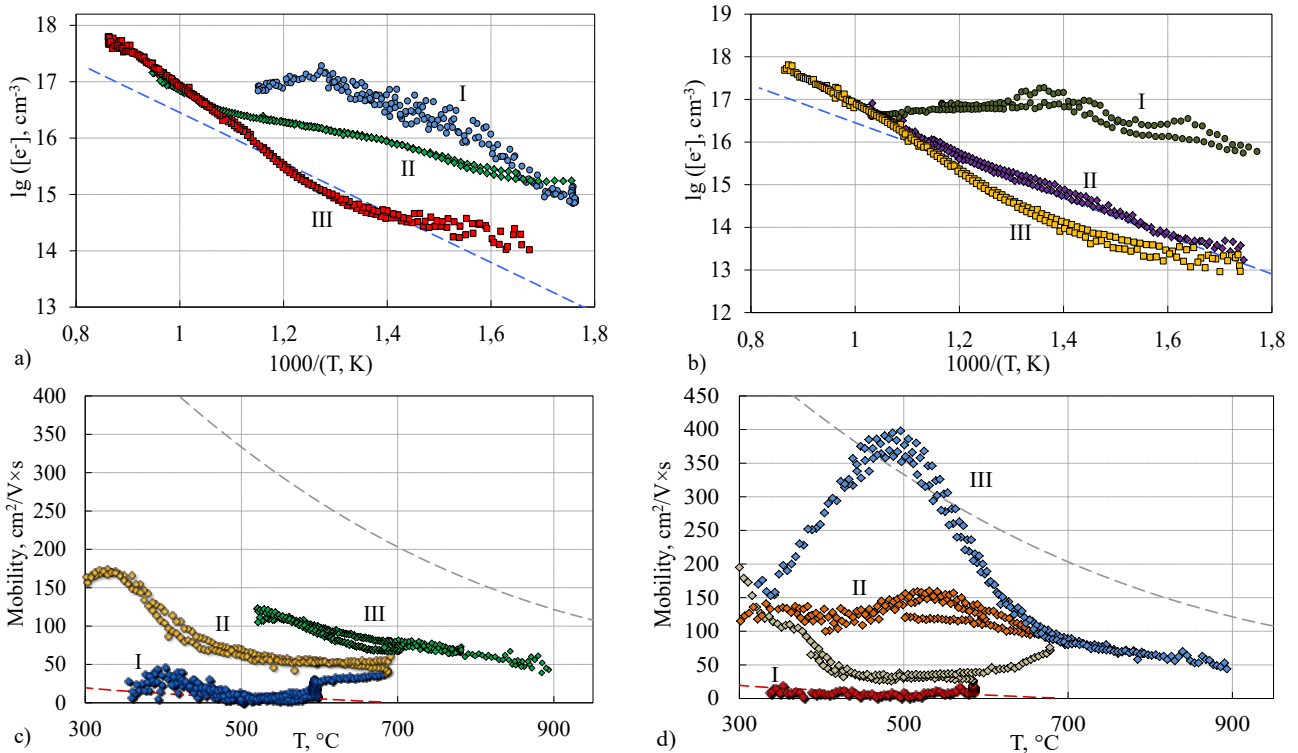


Figure 6. Temperature dependencies of concentration (a, b) and the charge-carrier mobility (c, d) in  $\text{Cd}_{0.85}\text{Mn}_{0.10}\text{Zn}_{0.05}\text{Te}$  (a, c) and  $\text{Cd}_{0.85}\text{Mn}_{0.10}\text{Zn}_{0.05}\text{Te:In}$  (b, d) at  $P_{\text{Cd}}$ , max. The dashed lines in (a-b) are the intrinsic carrier concentration in undoped CdTe; in (c-d) the dashed lines represent a modeling for hole mobility (lower red line) and electron mobility (upper grey line) in undoped CdTe. The numbers of curves (I, II, III) indicate the samples thermocycling order (see text).

At the following cycles of heating up to 700 °C, the concentration of electrons is reduced by one and two orders of magnitude in the  $\text{Cd}_{0.85}\text{Mn}_{0.10}\text{Zn}_{0.05}\text{Te}$  and  $\text{Cd}_{0.85}\text{Mn}_{0.10}\text{Zn}_{0.05}\text{Te}:\text{In}$  samples, respectively (Region II). At the same time, in the first sample the value of the carrier concentration was much higher than for undoped CdTe. For the second sample, the experimental data coincided with the theoretical line. After heating up to 900 °C (Region III), the concentration of charge carriers in  $\text{Cd}_{0.85}\text{Mn}_{0.10}\text{Zn}_{0.05}\text{Te}$  decreased again and became closer to the line of the intrinsic carrier concentration in undoped CdTe. Meanwhile as in  $\text{Cd}_{0.85}\text{Mn}_{0.10}\text{Zn}_{0.05}\text{Te}:\text{In}$ , these values were lower than the theoretical line (Region III). In addition, from Fig. 6 (c-d) we can see that during the measurements, the mobility of charge carriers in the samples also changed. In contrast to  $[e^-]$ , the mobility increased with the following cycles of heating and cooling. In general, the changes of mobility can be divided into three stages (Regions I-III in Figure 6, c and d). Initially, the measured mobility values obtained for both samples were similar to the modeling results for the hole mobility in undoped CdTe. Such low mobility values were kept until the next heating up to 700 °C, and then they increased to  $50 \text{ cm}^2/\text{V}\times\text{s}$  in  $\text{Cd}_{0.85}\text{Mn}_{0.10}\text{Zn}_{0.05}\text{Te}$  and to  $120\text{-}150 \text{ cm}^2/\text{V}\times\text{s}$  in  $\text{Cd}_{0.85}\text{Mn}_{0.10}\text{Zn}_{0.05}\text{Te}:\text{In}$  (Region II). At the time of heating up to 900 °C, the mobility again increased and held at  $50\text{-}120 \text{ cm}^2/\text{V}\times\text{s}$  over the temperature range of 500-900 °C for  $\text{Cd}_{0.85}\text{Mn}_{0.10}\text{Zn}_{0.05}\text{Te}$  (Fig.6 c, Region III). In the case of  $\text{Cd}_{0.85}\text{Mn}_{0.10}\text{Zn}_{0.05}\text{Te}:\text{In}$  (Fig. 6d, Region III) in the temperature range of 900-650 °C, the mobility values were at a level of  $50\text{-}100 \text{ cm}^2/\text{V}\times\text{s}$  and passed through the maximum ( $400 \text{ cm}^2/\text{V}\times\text{s}$ ) at 490 °C. In all three cases (Regions I-III), the mobility of the charge carriers was  $\sim 150 \text{ cm}^2/\text{V}\times\text{s}$  after cooling to 300 °C. Comparing the data from Figs. 6(a-b) and (c-d), we can see that each region of decrease in the charge carrier concentration corresponds to an increase of mobility.

The dependence of the electrical conductivity on temperature throughout all times for the high-temperature Hall-effect measurements for  $\text{Cd}_{0.85}\text{Mn}_{0.10}\text{Zn}_{0.05}\text{Te}$  and  $\text{Cd}_{0.85}\text{Mn}_{0.10}\text{Zn}_{0.05}\text{Te}:\text{In}$  are shown in Figures 7a and b, correspondingly. As we can see, according to the decreasing of charge-carrier concentration in both samples (Fig. 6, a-b) the electrical conductivity decreased. As a result, the resistivity of the investigated samples increased by two orders of magnitude from  $10^4$  to  $10^6 \text{ Ohm}\times\text{cm}$  (Fig. 5). Obviously the thermal treatment under Cd overpressure causes some restructuring of the point-defect system in the  $\text{Cd}_{1-x}\text{Mn}_x\text{Zn}_y\text{Te}$  crystal lattice.

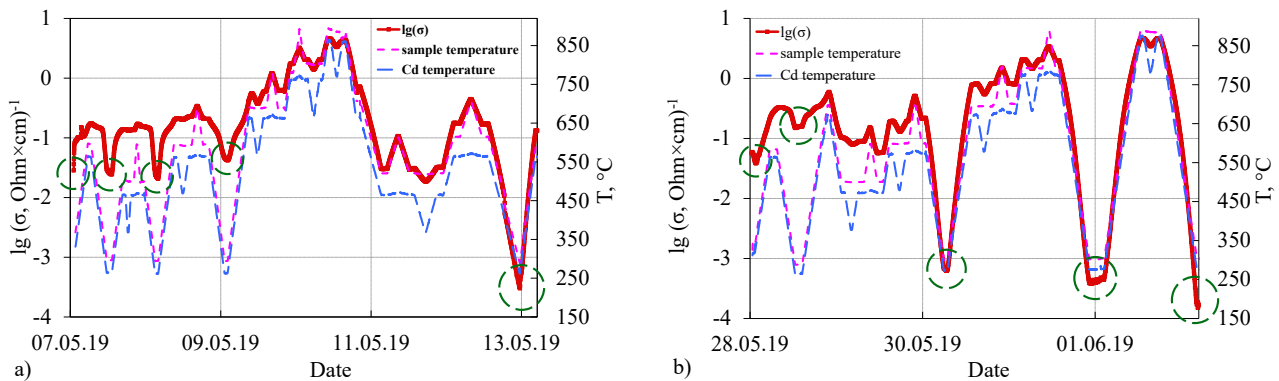


Fig. 7. Time-dependence of the electrical conductivity of  $\text{Cd}_{0.85}\text{Mn}_{0.10}\text{Zn}_{0.05}\text{Te}$  (a) and  $\text{Cd}_{0.85}\text{Mn}_{0.10}\text{Zn}_{0.05}\text{Te}:\text{In}$  (b) samples during High-Temperature Hall-effect measurements.

Studying the isobaric dependences of the charge-carrier concentration on the temperature, we can determine the total enthalpy of electron generation ( $\Delta H$ ) from the slope of experimental lines for established thermodynamic conditions (Fig. 8). For undoped  $\text{Cd}_{0.85}\text{Mn}_{0.10}\text{Zn}_{0.05}\text{Te}$  (Fig. 8a), the  $\Delta H$  values were significantly higher than for  $\text{Cd}_{0.85}\text{Mn}_{0.10}\text{Zn}_{0.05}\text{Te}:\text{In}$  crystal doped by indium (Fig. 8, b), especially at 0.01 atm. and 0.1 atm. (1.12 eV, 0.99 eV and 0.7 eV, 0.88 eV, respectively). Evidently, in the temperature range of 500-700 °C under low Cd vapor pressure, the donor impurity of indium plays a major role and controls the concentration of charge carriers. At higher temperatures and Cd pressure (700-900 °C, 0.3-1 atm.), the total enthalpy of the charge carrier generation for  $\text{Cd}_{0.85}\text{Mn}_{0.10}\text{Zn}_{0.05}\text{Te}$  was close to the  $\text{Cd}_{0.85}\text{Mn}_{0.10}\text{Zn}_{0.05}\text{Te}:\text{In}$  value under these conditions (0.83 eV, 0.93 eV and 0.84 eV, 0.87 eV for 0.3 and 1 atm., respectively). We can assume that the intrinsic conductivity of the material is dominated in this range. For both samples, the charge-carrier concentrations were below the line for intrinsic carrier concentration in undoped CdTe over all temperature and pressure ranges of the measurement.

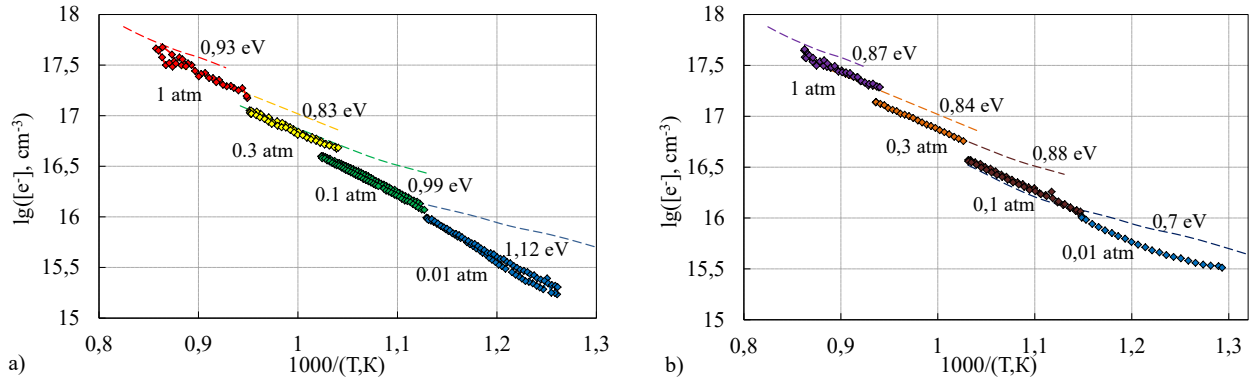


Figure 8. Temperature-dependence of charge-carrier density in  $\text{Cd}_{0.85}\text{Mn}_{0.10}\text{Zn}_{0.05}\text{Te}$  (a) and  $\text{Cd}_{0.85}\text{Mn}_{0.10}\text{Zn}_{0.05}\text{Te}:\text{In}$  (b) at constant Cd pressure. The dashed lines illustrate the electron density in undoped CdTe.

The obtained isotherms at constant temperatures of 500 and 600 °C have slopes close to 0 in both samples (Fig. 9). At 700 and 800 °C, for  $\text{Cd}_{0.85}\text{Mn}_{0.10}\text{Zn}_{0.05}\text{Te}$  the slopes of the isotherms are 0.27 and 0.34, respectively, while for  $\text{Cd}_{0.85}\text{Mn}_{0.10}\text{Zn}_{0.05}\text{Te}:\text{In}$  the slopes of the isotherms are 0.23 and 0.26 for 700 and 800 °C, and 0.33 for 900 °C. When

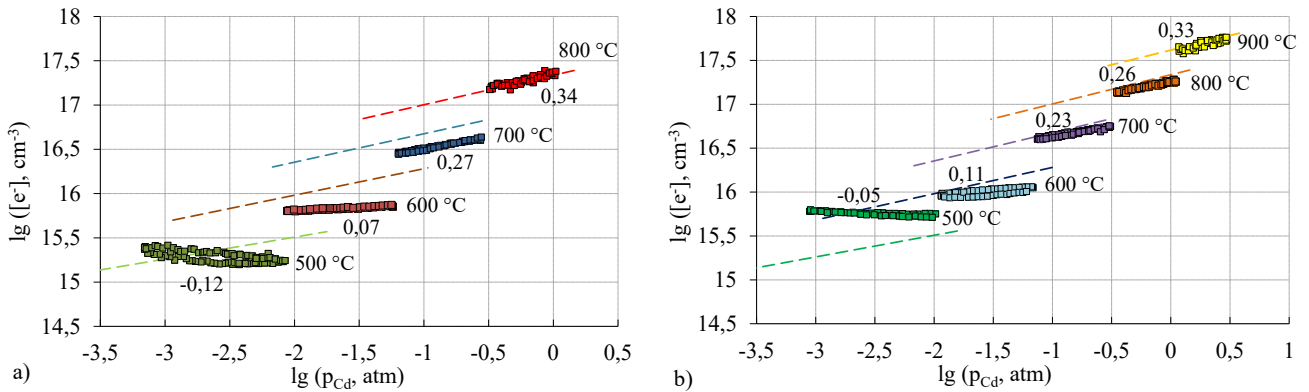


Fig. 9. Cadmium-vapor pressure dependence of the electron density in  $\text{Cd}_{0.85}\text{Mn}_{0.10}\text{Zn}_{0.05}\text{Te}$  (a) and  $\text{Cd}_{0.85}\text{Mn}_{0.10}\text{Zn}_{0.05}\text{Te}:\text{In}$  (b) samples at different constant temperatures. The dashed lines show similar dependencies for undoped CdTe.

comparing the data from Figs. 9a and b, we see that in the doped  $\text{Cd}_{0.85}\text{Mn}_{0.10}\text{Zn}_{0.05}\text{Te}:\text{In}$  sample, the isotherms at 500, 600 and 700 °C are situated higher than the isotherms in the undoped  $\text{Cd}_{0.85}\text{Mn}_{0.10}\text{Zn}_{0.05}\text{Te}$  sample. It can also indicate the role of the indium dopant.

#### 4. CONCLUSIONS

High temperature Hall-effect investigations were performed in this work to study the change of the concentration and mobility of charge carriers in  $\text{Cd}_{0.85}\text{Mn}_{0.10}\text{Zn}_{0.05}\text{Te}$  and  $\text{Cd}_{0.85}\text{Mn}_{0.10}\text{Zn}_{0.05}\text{Te}:\text{In}$  crystals grown by the vertical Bridgman technique. Previously we used IR observation, absorption measurements and current-voltage measurements for testing the crystal defect structure.

At lower temperatures and Cd vapor pressures (500-700 °C, 0.01 - 0.1 atm.) for undoped  $\text{Cd}_{0.85}\text{Mn}_{0.10}\text{Zn}_{0.05}\text{Te}$ , the total enthalpy of the electron generation values were higher than for  $\text{Cd}_{0.85}\text{Mn}_{0.10}\text{Zn}_{0.05}\text{Te}:\text{In}$  crystal doped by indium, indicating that the donor behavior of the indium impurity plays a major role and controls the concentration of charge carriers. At higher temperatures and Cd vapor pressures (700-900 °C, 0.3-1 atm.), the total enthalpy of charge-carrier generation for  $\text{Cd}_{0.85}\text{Mn}_{0.10}\text{Zn}_{0.05}\text{Te}$  was close to the  $\text{Cd}_{0.85}\text{Mn}_{0.10}\text{Zn}_{0.05}\text{Te}:\text{In}$  value for these conditions, demonstrating the intrinsic conductivity of the material. According to the decreasing charge-carrier concentration in both samples, a decrease in the electrical conductivity was observed. As a result, the resistivity of the investigated samples increased by two orders of magnitude from  $10^4$  to  $10^6$  Ohm $\times$ cm. Obviously the long thermal treatment under Cd overpressure causes

some rearrangement of the point-defect system in the crystal lattice of  $\text{Cd}_{1-x}\text{Mn}_x\text{Zn}_y\text{Te}$ , which needs more experimental data and theoretical calculations for a better understanding.

The obtained values of the band gap of  $\text{Cd}_{0.95-x}\text{Mn}_x\text{Zn}_{0.05}\text{Te}$  samples show a reasonable linear behavior as a function of the atomic fraction of Mn. It was shown that the value of the band gap of  $\text{Cd}_{0.90-x}\text{Mn}_{0.10}\text{Zn}_x\text{Te}$  increases with an increasing amount of Zn. We observed a decrease in the number of large Te inclusions and an increase in the number of small Te inclusions in both crystals after performing high-temperature Hall-effect measurements.

## REFERENCES

- [1] Kaushik, H. S., Anuradha Sharma and Mamta Sharma, "Dilute Magnetic Semiconductor: A Review of Theoretical Status," *IJIEASR* 3, 5-10 (2014).
- [2] Furdyna, J. K., "Diluted magnetic semiconductors," *J. Appl. Phys.* 64, R29-R64 (1988).
- [3] Nykoniuk, Ye., Solodin, S., Zakharuk, Z., Dremlyuzhenko, S., Rudyk, B., Fochuk, P., "Compensated donors in semi-insulating  $\text{Cd}_{1-x}\text{Mn}_x\text{Te}:\text{In}$  crystals," *J. Cryst. Growth* 500, 117-121 (2018).
- [4] Fochuk, P., Nakonechnyi, I., Kopach, O., Verzhak, Ye., Panchuk, O., Komar, V., Terzin, I., Kutnij, V., Rybka, A., Nykoniuk, Ye., Bolotnikov, A. E., Camarda, G. C., Cui, Y., Hossain, A., Kim, K. H., Yang, G., and James, R. B., "High-temperature treatment of In-doped CZT crystals grown by the high-pressure Bridgman method," *Proc. SPIE* 8507, 85071L-1-9 (2012).
- [5] Ben-Dor, L. and Yellin, N., "Vertical unseeded vapor growth and characterization of  $\text{Cd}_{0.95}\text{Zn}_{0.05}\text{Te}$  crystals," *J. Cryst. Growth* 71, 519-524 (1985).
- [6] Brovko, A. and Ruzin, A., "Study of material uniformity in high-resistivity  $\text{Cd}_{1-x}\text{Zn}_x\text{Te}$  and  $\text{Cd}_{1-x}\text{Mn}_x\text{Te}$  crystals," *Nucl. Instrum. Methods Phys. Res. A*, 1-3 (2019).
- [7] Qadri, S. B., Skelton, E. F., Webb, A. W., and Kennedy, J., "Structural studies of  $\text{Cd}_{0.95}\text{Zn}_{0.05}\text{Te}$  and  $\text{Cd}_{0.90}\text{Mn}_{0.10}\text{Te}$  under pressure," *J. Vac. Sci. & Technol. A* 4, 1971-1973 (1986).
- [8] Fochuk, P., Grill, R., Nakonechnyi, I., Kopach, O., Panchuk, O., Verzhak, Ye., Belas, E., Bolotnikov, A. E., Yang, G., and Jame, R. B., "Effect of  $\text{Cd}_{0.9}\text{Zn}_{0.1}\text{Te}:\text{In}$  Crystals Annealing on Their High-Temperature Electrical Properties," *IEEE Transactions on Nuclear Science* 58, 2346-2351 (2011).
- [9] Du Yuan-yuan, Jie Wan-qi, Zheng Xin, Wang Tao, Bai Xu-xu, and Yu Hui, "Growth interface of In-doped  $\text{CdMnTe}$  from Te solution with vertical Bridgman method under ACRT technique," *Trans. Nonferrous Met. Soc. China* 22, 143-147 (2012).
- [10] Vere, A.W., Cole, S., and Williams, D.J., "The origins of twinning in  $\text{CdTe}$ ," *J. Electron. Mater.* 12, 551-561 (1983).
- [11] Belas, E., Bugar, M., Grill, R., Franc, J., Moravec, P., Hlidek, P. and Hoschl, P., "Reduction of Inclusions in  $(\text{CdZn})\text{Te}$  and  $\text{CdTe}:\text{In}$  Single Crystals by Post-Growth Annealing," *J. Electron. Mater.* 37, 1212-1218 (2008).
- [12] Kopach, V., Kopach, O., Fochuk, P., Filonenko, S., Shcherbak, L., Bolotnikov, A. E. and James, R. B., "Vertical Bridgman growth and characterization of  $\text{Cd}_{0.95-x}\text{Mn}_x\text{Zn}_{0.05}\text{Te}$  ( $x=0.20, 0.30$ ) single-crystal ingots," *Proc. SPIE* 10392, 1039214-1-8 (2017).
- [13] Kopach, V., Kopach, O., Kanak, A., Shcherbak, L., Fochuk, P., Bolotnikov, A. E. and James, R. B., "Properties of  $\text{Cd}_{0.90-x}\text{Mn}_x\text{Zn}_{0.10}\text{Te}$  ( $x = 0.10, 0.20$ ) crystals grown by Vertical Bridgman method," *Proc. SPIE* 10762, 1076212-1-8 (2018).
- [14] Gad, S.A., Boshta, M., Moustafa, A.M., Abo El-Soud, A.M., Farag, B.S., "Structural, optical, magnetic and electrical properties of dilute magnetic semiconductor  $\text{Cd}_{1-x}\text{Mn}_x\text{Te}$ ," *Solid State Sciences* 13, 23-29 (2011).